The Interaction between Micrometer-size Particles and Flat Substrates: A Quantitative Study of Jump-to-Contact

B. Gady[a]; D. Schleef[a]; R. Reifenberger[a]; D. S. Rimai[b]

[a] Department of Physics, Purdue University, W. Lafayette, Indiana, USA [b] Office Imaging Research and Technology Development, Eastman Kodak Company, Rochester, New York, USA

PLEASE SCROLL DOWN FOR ARTICLE

The Interaction between Micrometer-size Particles and Flat Substrates: A Quantitative Study of Jump-to-Contact

B. GADY[a], D. SCHLEEF[a], R. REIFENBERGER[a,*] and D. S. RIMAI[b]

[a] *Purdue University, Department of Physics, W. Lafayette Indiana 47907, USA;*
[b] *Office Imaging Research and Technology Development,
Eastman Kodak Company, Rochester, New York 14653-6402, USA*

The interaction force acting on an individual micrometer-size polystyrene particle near a flat, electrically conducting substrate has been measured by attaching the particle to an atomic force microscope cantilever. From the spatial dependence of the interaction force, the equations of motion governing a particle near the substrate can be determined. These considerations allow a prediction of the jump-to-contact distance of the particle as it approaches the substrate. This distance is measured as a function of particle radius and compared with predictions based on the relevant interaction force models.

Keywords: Particle adhesion; atomic force microscope (AFM); surface force interaction; jump-to-contact

1. INTRODUCTION

To understand better the mechanisms controlling adhesion of micrometer-size particles to substrates, it is necessary to perform experiments that characterize the interaction forces acting on a particle as the particle approaches a substrate. As shown previously [1 – 5], this experiment can be performed by attaching an individual micrometer-size particle to an atomic force cantilever. The ability of an atomic

---

*Corresponding author.

force microscope (AFM) to measure small deflections of the cantilever accurately makes it an ideal tool for probing the particle-substrate interaction. The high degree of control inherent in such an experiment allows for the determination of many important parameters governing the particle-substrate interaction.

Using the AFM configuration, the force acting on a particle is inferred from the measured deflection of a cantilever with a known spring constant k. An experiment in which the particle is loaded and then unloaded from the substrate is referred to as a force curve. The force curve can be classified into five separate regimes that are labeled by the segments (a) through (e) in Figure 1.

Initially, the particle is assumed to be sufficiently far from the substrate so as not to be influenced by it. As the surface-to-surface separation is decreased, any forces acting between the particle and substrate cause a deflection of the cantilever (segment (a) in Fig. 1). The spatial dependence of this deflection is useful for identifying the origin of the interaction force [6]. When the particle is only a few tens of nanometers from the substrate, an instability arises and the particle jumps into contact with the substrate (segment (b) in Fig. 1). After contact is made, a controlled loading and unloading of the particle against the substrate can be performed (segment (c) Fig. 1). Because

Force Curve

jump-to-contact
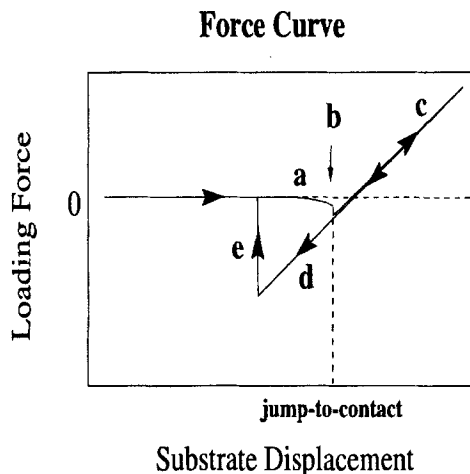
Substrate Displacement

FIGURE 1   Schematic force curve between a micrometer-size particle and flat substrate showing five separate segments labeled by the letters (a) thru (e).

the maximum applied load can be controlled in a straightforward way, a quantitative determination of the importance of elastic and inelastic processes can result. Upon unloading, the adhesive properties of the particle-substrate can be investigated (segment (d) Fig. 1). The work of removal as well as the lift-off force (segment (e) Fig. 1) can then be determined. One major advantage of the AFM technique is that systematic and controlled experiments can be performed as a function of particle size and substrate composition. In this way, important information about the adhesive properties of different particle/ substrate systems can be investigated.

As examples of the type of information obtained from previous AFM studies, Gady et al. [5] have carefully investigated the region of the force curve labeled by segment (a) in Figure 1. By determining the force acting on a polystyrene particle by directly measuring the deflection of the AFM cantilever, or by using oscillating cantilever techniques to measure the force gradient, considerable information about the forces acting on the particle was obtained. Both a van der Waals and localized electrostatic (or "charged patch" [7]) contribution to the interaction force were identified. In subsequent studies, a better characterization of the electrostatic contribution to the interaction force was completed, allowing for a quantitative estimate of the charge transfer between the particle and substrate [6]. Schaefer et al. [1] investigated the compressive region of the force curve and estimated the amount of deformation of a spherical polystyrene particle. In addition, a study to determine whether a variable loading force produced any significant change in the lift-off force of a polystyrene particle from a p-type Si substrate was also reported [1].

Schaefer et al. [4] also investigated the adhesion forces by system-atically measuring the force required to remove different particles from a variety of substrates. In this study, the relative lift-off forces were found to scale with the relative works of adhesion in a manner qualitatively consistent with the predictions of the Johnson, Kendall, Roberts (JKR) theory of adhesion [8]. The absolute magnitude of the lift-off force was found to be smaller than expected, an effect that was attributed to the surface roughness of the particle as determined from AFM images of the particle surface. Although most of these studies mentioned above have been confined to well-characterized, spherical particles and atomically-flat substrates, the results obtained indicate

that the AFM techniques and methods developed are capable of providing useful, quantitative information about particulate adhesion that is difficult to ascertain using more conventional approaches.

An important aspect of the force curve that has not yet been carefully analyzed in particle adhesion experiments is the jump-to-contact (segment (b) in Fig. 1). As shown in Figure 2(a), at infinite separation distance there is no attractive force between the particle and the substrate; however, the cantilever experiences an increasingly attractive force as the separation distance between the particle and substrate decreases as shown in Figure 2(b). An instability results at a point where the cantilever can no longer compensate for the interaction force between the particle and substrate. At this point, a sudden jump-to-contact of the particle to the substrate occurs.

In order to predict the point of instability when jump-to-contact occurs, it is necessary to know in some detail the spatial dependence of the interaction force that the particle experiences. By measuring the jump-to-contact distance as a function of sphere radius, a further test of the interaction force between particle and substrate will result. In what follows, we have analyzed the jump-to-contact region, taking into account the effects of both van der Waals and electrostatic forces on this phenomenon. We show that systematic measurements of the separation distance at which jump-to-contact occurs can be quantita-
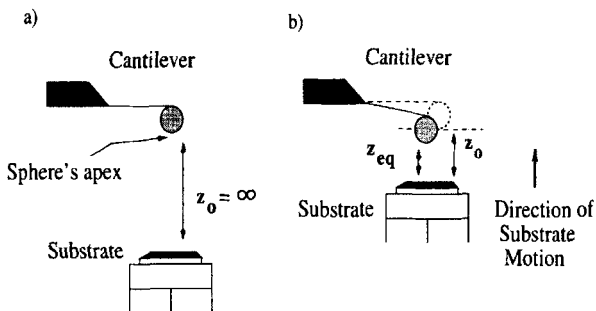
FIGURE 2 A schematic depicting the deflection of cantilever because of particle-substrate interaction. In (a), the surface-to-surface separation between the particle and conducting substrate is assumed to be infinite and no interaction results. In (b), the substrate has been moved closer to the particle and the particle experiences a force, causing a deflection of the cantilever from its original position. Under these conditions, the equilibrium surface-to-surface separation is denoted by z_{eq}.

tively understood using reasonable models for the interaction force between the particle and substrate.

2. EXPERIMENTAL CONSIDERATIONS

The particles used in these experiments were well-characterized polystyrene spheres of different size. Each particle was mounted on the edge of AFM cantilevers [9] using a microscopic drop of Norland Optical Cement No. 68 applied to the cantilever. Experiments have shown that this cement remains viscous for a sufficiently long time to position the sphere accurately in the cement with the aid of a micromanipulator. The particle was pressed into the cement to allow close contact of the particle with the cantilever. As discussed previously, the cement was cured by exposure to UV light for approximately 10–15 min [4]. After curing, the sphere and cantilever were mounted inside a home-built AFM system, which was located inside a small, stainless steel chamber [4]. Detection of the cantilever displacement as a function of the sphere-substrate separation distance was done using a laser deflection method and phase sensitive detection [10–12]. A 68030 CPU-based computer system, similar to that described previously [13], controlled the experiment. The spring constants of all cantilevers were independently calibrated by measuring the resonance frequency of the bare cantilevers, as discussed elsewhere [14]. To avoid problems with adsorbed layers of water, all measurements were performed in a partial vacuum of ~20 m Torr after purging the system repeatedly with dry nitrogen. The conducting substrates were freshly-cleaved samples of highly-oriented pyrolitic graphite (HOPG).

The polystyrene spheres used in this study were formed by a process known as "limited coalescence". A monomer is dispersed in a non-polar solvent such as hexane and the polymer is formed by blending in a chemical initiator which forms free radicals at the ends of the chain. There is also a reaction terminator, which will react with free radical ends to terminate the reaction. Obviously, the longer the chains, the fewer the chain ends available so the higher the probability that the terminator will stop the reaction. This limits the molecular weight of the polymer. The polymer solution is also dispersed in an aqueous

medium and would, therefore, tend to coalesce into a large mass. However, by adding sub-micrometer particles such as silica, the tendency to coalesce is limited. By varying the silica concentration, the size of the particles is controlled. After forming, the particles are dried and the silica is removed by washing in a concentrated solution of KOH. The spherical particles are then thoroughly rinsed to neutral pH in distilled water and dried.

3. THEORETICAL CONSIDERATIONS

3.1. Defining the Jump-to-Contact Distance

It is useful to understand the behavior of the lever as a function of the separation between particle and substrate for a particle mounted on a cantilever with a known spring constant. As the particle approaches the substrate, the cantilever will experience a displacement as a result of the vector sum of all the interaction forces which, from prior studies [5, 6], are thought to contain a van der Waals and an electrostatic contribution. It follows that if the surface-to-surface separation is initially set to some value z_o, the cantilever will deflect to a new position, z_{eq}, such that the Hooke's law restoring force

$$F_{\text{restoring}} = k\left(z_{eq} - z_o\right) \tag{1}$$

is equal to and opposite the net interaction force between the particle and substrate.

This situation is illustrated in Figure 3, which depicts (i) the functional form of a representative long-range interaction force (dashed line) acting on the particle and (ii) the summation of this interaction force with the cantilever's restoring force (solid line). In this example, the equilibrium surface-to-surface distance between the particle and substrate, z_{eq} (see diamond), is shown assuming an initial surface-to-surface separation between particle and substrate of $z_o = 20$ nm. It is evident from Figure 3 that for small displacements of the particle about z_{eq} the motion is harmonic and the restoring force is linear with displacement.

The location of z_{eq} depends on the spring constant of the cantilever and the nature of the interaction force. The effect for different spring
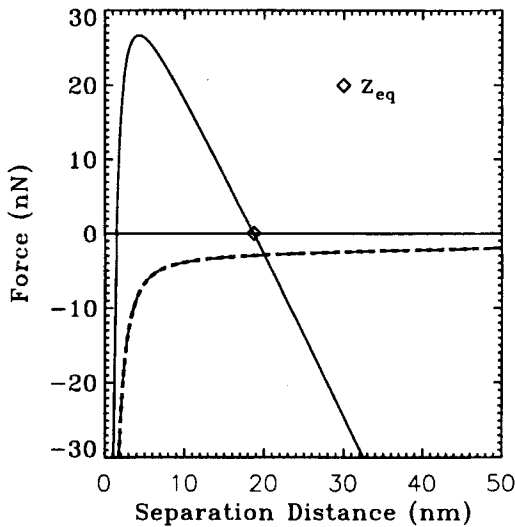
FIGURE 3   A schematic plot illustrating the interaction force (dotted line) and the sum of the interaction force and the cantilever restoring force (solid line) as a function of the separation distance between a particle and flat conducting substrate. In this plot, the particle is attached to a cantilever with a 2 N/m spring constant. The equilibrium position of the particle (z_{eq}), when placed at a surface-to-surface separation of 20 nm, is indicated by the position of the diamond.

constants is illustrated in Figure 4 for a variety of different cantilevers commonly used in AFM studies. This figure illustrates how the equilibrium separation of a 3 μm radius particle, set initially to a surface-to-surface separation $z_o = 80$ nm, would vary with cantilever spring constant.

There is a well-defined position where the cantilever becomes unstable. This point of instability, defined as the jump-to-contact distance, is determined by two conditions: both the net force *and* the net force gradient between the particle and substrate must sum to zero. These conditions are given by

$$F_{net} = F_{restoring} + F_{interaction} = 0 \qquad (2)$$

and

$$F'_{net} = F'_{restoring} + F'_{interaction} = 0. \qquad (3)$$
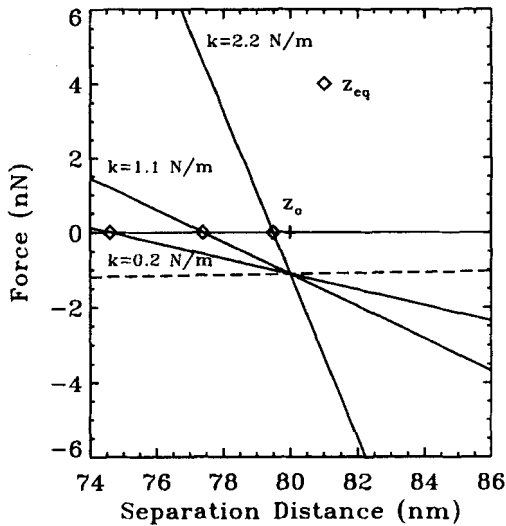
B. GADY *et al.*

FIGURE 4   Variation of the cantilever deflection due to an attractive interaction force. The solid lines are the net interaction for varying cantilever stiffness. The spring constants are 0.2 N/m, 1.1 N/m, and 2.2 N/m. The net interaction is due to a sum of a van der Waals force and an electrostatic force between a 3 μm sphere and grounded plane (dashed line). The charge is specified by 1.3×10^{-17} C distributed uniformly over a ∼ 100 nm radius. The initial surface-to-surfce separation (with no forces present) is set to 80 nm. The points marked by diamonds indicate the equilibrium position of each cantilever in the presence of the interaction force.

These two conditions can be understood graphically as shown in Figure 5. As z_o is decreased, the linear restoring force supplied by the cantilever for a stable situation must continually increase. Eventually, an unstable situation occurs. In Figure 5, this point is located at z_{jump}, a separation distance where both the net force and the net force gradient simultaneously become zero. At z_{jump}, the cantilever will deflect uncontrollably towards the substrate to find an equilibrium position. However, because the equilibrium position now coincides with a maximum in the force curve, the particle will jump into contact with the substrate. The combination of these conditions specified in Eqs. (2) and (3), therefore, determines the jump-to-contact distance. The above discussion is intentionally general. It is worthwhile to calculate the jump-to-contact distance assuming a few specific models for the interaction force.
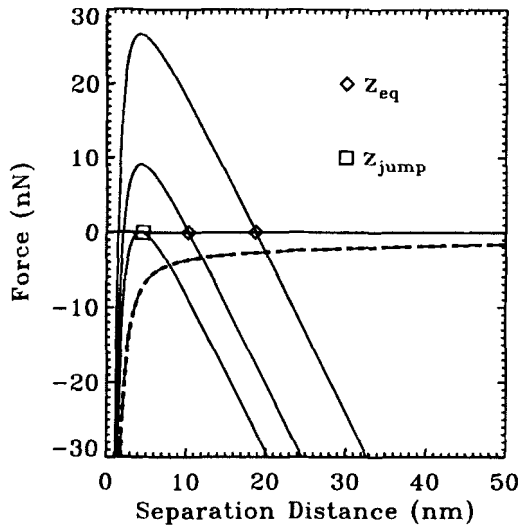
FIGURE 5 The attractive interaction force acting on a particle (dashed line) is modified by the cantilever restoring force to produce the net interaction force (solid lines) for three different surface-to-surface separations. As the separation distance between the particle and substrate decreases, the net interaction force evolves as shown. The points indicated by diamonds show the equilibrium position for two different particle-substrate separations. The point indicated by the square shows where the equilibrium position is unstable and the jump-to-contact occurs.

3.2. Including the van der Waals Force

If the interaction force is solely determined by a van der Waals interaction characterized by a sphere-plane geometry, the jump-to-contact separation can be analytically calculated. For a sphere of radius R attached to a cantilever with spring constant k having a surface-to-surface separation z_{eq} from a planar substrate, we have

$$F_{net} = k\left(z_o - z_{eq}\right) - \frac{HR}{6z_{eq}^2} = 0 \qquad (4)$$

and

$$F'_{net} = \frac{\partial F_{net}}{\partial z_{eq}} = -k + \frac{HR}{3\,z_{eq}^3} = 0 \qquad (5)$$

In these equations, H is the Hamaker constant that characterizes the van der Waals interaction between the sphere and substrate.

The jump-to-contact distance, z_{jump}, is determined from these two conditions. Equations (4) and (5) are simultaneously satisfied when

$$z_o = \frac{3}{2} z_{eq} \equiv z_{jump} \qquad (6)$$

In order to determine the jump-to-contact distance, z_{jump}, the value of z_{eq} from Eq. (5) is substituted into Eq. (6), giving

$$z_{jump} = \frac{3}{2} \left(\frac{HR}{3k} \right)^{1/3} \qquad (7)$$

This defines the surface-to-surface separation below which no interaction force can be measured. The jump-to-contact distance depends on the parameters determining the interaction force between the particle and substrate and should scale as $R^{1/3}$ where R is the particle radius.

3.3. Including the Electrostatic Force

A second model for the interaction force includes an electrostatic contribution. As found in previous studies [5, 6], an electrostatic force can arise due to contact charging of the particle with the substrate. Typically, after a polystyrene sphere is mounted to a cantilever, inserted into the force apparatus, and brought into contact with an HOPG substrate, the sphere is found to acquire a net charge of $\sim(1-10) \times 10^{-17} C$ (typically, a few hundred electrons). Subsequent contact of the sphere to the substrate increases the charge by a few electrons/contact. Under these conditions, the details of the interaction force depends on how the charge is distributed on the particle and substrate.

Prior studies have provided some insight into this interesting and important problem. According to the JKR model for adhesion [8], upon contact, a spherical particle of radius R will form a small contact area with the surface. If this small region of the dielectric sphere becomes triboelectrically charged, an electrostatic force between the sphere and grounded substrate will occur. The long-range interaction

force which arises can influence the subsequent jump-to-contact behavior and, therefore, must be taken into account. The electrostatic force has been modeled under these circumstances. Prior data suggest that the charge transferred to the sphere is trapped near the sphere's apex and distributed over a spherical region having a radius R_{eff} much smaller than the sphere's radius R. This assumption is reasonable since the contact radius of the sphere with the substrate, a_{jkr}, under zero load is given by the well-known result [8]

$$a_{jkr} = \left(\frac{6\pi R^2 W}{K}\right)^{1/3} \tag{8}$$

where R is the sphere's radius, W is the work of adhesion given by

$$W = \gamma_{\text{sphere}} + \gamma_{\text{substrate}} - \gamma_{12} \tag{9}$$

where γ_{12} is approximated by $2\sqrt{\gamma_{\text{sphere}}\gamma_{\text{substrate}}}$, and γ_{sphere} and $\gamma_{\text{substrate}}$ are the surface-free energies of the sphere and substrate, respectively. The parameter K in Eq. (8) accounts for the elastic properties of the sphere and substrate and is given by

$$K = \frac{4}{3}\left(\frac{1 - \nu_{\text{sp}}^2}{E_{\text{sp}}} + \frac{1 - \nu_{\text{sub}}^2}{E_{\text{sub}}}\right)^{-1} \tag{10}$$

Here, ν_{sp} and ν_{sub} are the Poisson ratios of the sphere and substrate, respectively, and E_{sub} and E_{sp} are the Young's moduli for the substrate and sphere, respectively. As an example, for a 3 μm radius polystyrene sphere on graphite under zero load, we find that $a_{jkr} \simeq 160$ nm. This is in reasonable agreement with the experimentally-determined contact radius of similar particles on silicon substrates [15] and suggests that any charge transferred during contact of an insulating particle against a conducting substrate will be trapped at the sphere's apex in a region specified by an effective radius R_{eff} that is comparable with a_{jkr}.

As discussed elsewhere, the observed charging of a micrometer-size polystyrene sphere is consistent with electron transfer into trap states in the polystyrene sphere upon contact with highly-oriented pyrolitic graphite (HOPG) substrate [5, 6]. Experiment shows that most of the states fill upon initial contact with the substrate. Subsequent contacts

give rise to a small linear increase in the amount of charge transferred [5, 6].

The distribution of the charge, Q, transferred is of considerable interest. We find that the spatial dependence of the resulting interaction force data can be explained if it is assumed that this charge is trapped in a spherical region having a radius comparable with a_{jkr}. The data cannot be explained by a charge uniformly distributed on the sphere. At this point, the consequences of other possible localized distributions in the charge have not yet been explored.

For the geometry employed in these studies, a_{jkr} calculated from Eq. (8) is much smaller than the radius, R, of the sphere. Under these circumstances, we use an image force between the spherically-charged region on the particle's apex to approximate the electrostatic force produced by the conducting substrate, giving [5, 6]

$$F_{\text{net}} = k\left(z - z_{\text{eq}}\right) - \frac{HR}{6\,z_{\text{eq}}^2} - \frac{Q^2}{16\,\pi\,\varepsilon_o\left(z_{\text{eq}} + a_{jkr}\right)^2} = 0 \qquad (11)$$

and

$$F'_{\text{net}} = -k + \frac{HR}{3\,z_{\text{eq}}^3} + \frac{Q^2}{8\,\pi\,\varepsilon_o\left(z_{\text{eq}} + a_{jkr}\right)^3} = 0 \qquad (12)$$

The jump-to-contact distance may be approximated by realizing that the contact radius is much larger than the surface-to-surface separation between the two surfaces just prior to the jump, *i.e.*, $a_{jkr} \gg z_{\text{eq}}$. The relations for the net force and the net force gradient then become

$$F_{\text{net}} \approx k\left(z - z_{\text{eq}}\right) - \frac{HR}{6\,z_{\text{eq}}^2} - \frac{Q^2}{16\,\pi\,\varepsilon_o\left(a_{jkr}\right)^2} = 0 \qquad (13)$$

and

$$F'_{\text{net}} \approx -k + \frac{HR}{3\,z_{\text{eq}}^3} + \frac{Q^2}{8\,\pi\,\varepsilon_o\left(a_{jkr}\right)^3} = 0 \qquad (14)$$

In which case,

$$z_{jump} \approx \frac{3}{2} \left(\frac{HR}{3\,k'} \right)^{1/3} \tag{15}$$

where $k' = [k - Q^2/(8\,\pi\,\varepsilon_o\,a_{jkr}^3)]$. Eq. 15 provides a basis to estimate the jump-to-contact distance when electrostatic forces are important.

4. RESULTS

A comparison between the experimentally-measured jump-to-contact distance as a function of sphere radius with Eq. (7) (van der Waals force) and Eq. (15) (van der Waals force plus an electrostatic contribution), is given in Figure 6. The data were accumulated over a three-year period of time as the interaction force between different polystyrene spheres and HOPG substrates were measured. The error bars represent the standard deviation in the jump-to-contact distances measured. For the larger particles, at least five independent measurements were averaged to obtain the data point plotted. For the smallest sphere (radius of 2 μm), only two measurements were available. Taken together, these data provide information about the systematic functional dependence on the jump-to-contact distance as a function of particle size.

The data indicate that a van der Waals contribution *alone* cannot explain the measured jump-to-contact distance. An electrostatic contribution is required to obtain a reasonable quantitative fit to the data. This electrostatic contribution is approximated by a net charge on each sphere of about 500 electrons. Since only Q^2 enters the force equation, the polarity of the charge transfered cannot be determined from this analysis. This amount of charge transfer is consistent with values of charge measured after the initial contact of a polystyrene sphere with HOPG found in previous studies [5, 6]. When the data are analyzed in more detail, the functional dependence of the lift-off force appears to be consistent with the $R^{1/3}$ dependence predicted by the simple theory outlined above. Data taken over a wider range of sphere radii are needed before a firm conclusion about this particular issue can be reached.
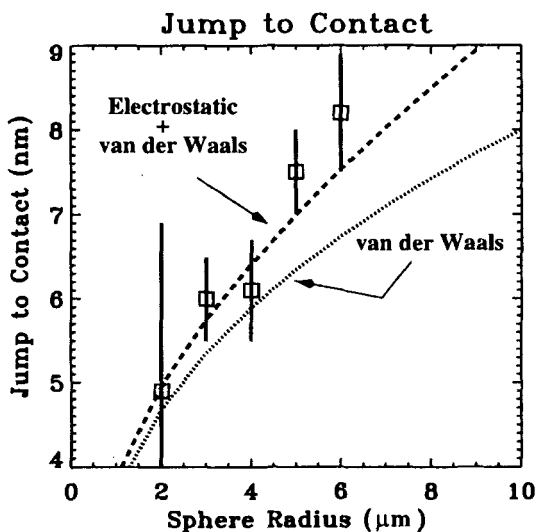
Jump to Contact

FIGURE 6   Jump-to-contact data (squares) plotted as a function of the polystyrene sphere radius. A comparison is made between the case of a purely van der Waals force (Eq. (7); dotted line) and a van der Waals plus electrostatic interaction (Eq. (15); dashed line). The parameters used in calculating the van der Waals and electrostatic fits are $Q = 500$ electrons, $R_{eff} = a_{jkr}$, and $H = 0.6$ eV.

5. CONCLUSIONS

While a pure van der Waals interaction may result in a jump-to-contact distance of approximately one nanometer for a bare AFM tip, jump-to-contact distances on the order of five nanometers are found if a micrometer-size insulating sphere such as polystyrene is attached to an AFM cantilever. In order to understand this result, a simple thoery of the jump-to-contact distance has been developed. Measurements of the jump-to-contact distance are found to be consistent with the *same* interaction force model required to fit cantilever deflection data obtained as a function of the surface-to-surface particle-substrate separation. The measured jump-to-contact distance is consistent with an interaction force model containing both van der Waals and a localized electrostatic force. The reasonable agreement between the jump-to-contact data and theoretical expectations provides further confidence about the validity of the force model to represent the

interaction between micrometer-size particles and flat conducting substrates.

Acknowledgement

References

[1] Schaefer, D. M., Carpenter, M., Reifenberger, R., DeMejo, L. P. and Rimai, D. S., *J. Adhesion Sci. Tech.* **8**, 197 (1994).
[2] Mizes, H. A., *J. Adhesion Sci. Tech.* **8**, 937 (1994).
[3] Ott, M. L. and Mizes, H. A., *Colloids Surf. A* **87**, 245 (1994).
[4] Schaefer, D. M., Carpenter, M., Gady, B., Reifenberger, R., DeMejo, L. P. and Rimai, D. S., *J. Adhesion Sci. Tech.* **9**, 1049 (1995).
[5] Gady, B., Schleef, D., Reifenberger, R., DeMejo, L. P. and Rimai, D. S., *Phys. Rev.* **B53**, 8065 (1996).
[6] Gady, B., Reifenberger, R., Rimai, D. S. and DeMejo, L. P., *Langmuir* **13**, 2533 (1997).
[7] Hays, D. A., "Adhesion of charged particles", in *Fundamentals of Adhesion and Interfaces* D. S. Rimai, L. P. DeMejo and K. L. Mittal, Eds. (VSP, Utrecht, 1995), pp. 61–71.
[8] Johnson, K. L., Kendell, K. and Roberts, A. D., *Proc. R. Soc. London* **A324**, 301 (1971).
[9] Available from Park Scientific Instruments, Sunnyvale, CA 94089, USA.
[10] Meyer, G. and Amer, N. M., *Appl. Phys. Lett.* **53**, 1045 (1988).
[11] Meyer, G. and Amer, N. M., *Appl. Phys. Lett.* **53**, 2400 (1988).
[12] Alexander, S., Hellemans, L., Marti, O., Schneir, J., Elings, V., Hansma, P. K., Longmire, M. and Gurley, J., *J. Appl. Phys.* **65**, 164 (1989).
[13] Piner, R. and Reifenberger, R., *Rev. Sci. Instrum.* **60**, 3123 (1989).
[14] Cleveland, J. P., Manne, S., Bocek, D. and Hansma, P. K., *Rev. Sci. Instrum.* **64**, 403 (1993).
[15] Rimai, D. S., DeMejo, L. P. and Bowen, R. C., "Mechanics of particle adhesion", in *Fundamentals of Adhesion and Interfaces*, D. S. Rimai, L. P. DeMejo and K. L. Mittal, Eds. (VSP, Utrecht, 1995), pp. 1–23.